PHYSICAL REVIEW E **82**, 045201(R) (2010)

Target-wave to spiral-wave pattern transition in a discrete Belousov-Zhabotinsky reaction driven by inactive resin beads

Guanqun Wang,[1] Qingsheng Wang,[2,*] Peng He,[1] Srinivasa Pullela,[1] Manuel Marquez,[3,4] and Zhengdong Cheng[1,†]
[1]*Artie McFerrin Department of Chemical Engineering, Texas A&M University, College Station, Texas 77843-3122, USA*
[2]*Department of Fire Protection and Safety, Oklahoma State University, Stillwater, Oklahoma 74078-8016, USA*
[3]*YNano LLC, 14148 Riverdowns South Drive, Midlothian, Virginia 23113-3796, USA*
[4]*Escuela de Ingenierıas, Universidad de Malaga, C/Pedro Oritz Ramos, s/n 29071 Malaga, Spain*
(Received 22 June 2010; published 13 October 2010)

Wave pattern formation and transition in chemical and biochemical reaction systems can reveal the system properties. We investigate the pattern transition from target waves to spiral waves upon the increment of inactive beads in a discrete system model, where ion-exchange resin loaded with Belousov-Zhabotinsky catalyst corresponds to the active beads. The results show that inactive beads slow the propagation speed of target waves and increase the wave frequency. As the population of inactive beads increases, clusters are formed, which then break waves into segments where bounded spiral pairs are generated and separated into individual spirals. From this observation, we conclude that the population of inactive resin beads acts as the bifurcation parameter controlling the wave pattern transition from targets to spirals.

DOI: 10.1103/PhysRevE.82.045201 PACS number(s): 89.75.Kd, 82.40.Bj, 47.54.−r, 05.45.−a

I. INTRODUCTION

Spiral and target waves appear spontaneously in biological excitable media (e.g., heart tissue [1–3]), in disordered media [4], and in nonlinear chemical reactions (e.g., the Belousov-Zhabotinsky (BZ) reaction [5,6]). Wave pattern transition phenomena in excitable media reveal how dynamics are organized in a system [7,8]. Due to the heterogeneities of biological systems, discrete systems with nonlinear chemical elements would be closely related analogs [9–11]. Research on nonlinear waves in discrete systems, however, is less common than that on homogeneous excitable media [5,6]. Inactive elements, specifically, heterogeneous features, frequently exist in discrete excitable systems. For example, fibrotic nonexcitable "dead" tissue normally presents at a small percentage of normal heart tissue. As a result of aging, after a myocardial infarction (heart attack), or in the case of cardiac myopathies, the percentage of fibrotic tissue increases dramatically, up to 30–40 % [12,13].

Interesting observations show that there is a wave-form change from plane wave to multiple spiral wavelets accompanying the procession from normal sinus rhythm to ventricular tachycardia, and finally to ventricular fibrillation [14]. Also, in a monolayer of chick embryonic heart cells, transition has been observed from target to spiral waves [7]. Both wave pattern transitions might be caused by increased heterogeneities of the environment on which the wave patterns are generated and propagated, but the mechanism which gives rise to arrhythmias is still not clear. Insight into the dynamics of spirals in bioexcitable media and the understanding of the genesis of spiral waves and their interactions would offer insight into the development of effective approaches to interrupt arrhythmias. In this Rapid Communication, we address such wave pattern transitions using a simple heterogeneous BZ reaction as a system model. Due to the poor understanding of the transition between different wave patterns, it would be of great interest to investigate how the wave pattern transition is driven by inactive resin beads.

II. EXPERIMENTS

Belousov-Zhabotinsky active beads were fabricated by immersion of polystyrene ion-exchange beads (Acros Organics, Morris Plains, NJ) in a 0.025 M aqueous solution of ferroin (Sigma-Aldrich, Milwaukee, WI) in a capped glass bottle. Ferroin, with the molecular formula as $[Fe(o\text{-}phen)_3]SO_4$, where o-phen is an abbreviation for 1,10-phenanthroline, serves as the catalyst for BZ reactions. The loading of ferroin into the resin beads was completed in 10 h, yielding a colorless solution. The beads were then filtered and dried in an oven at 50 °C overnight. The concentration of catalyst in active beads was 25 μmol/g based on the assumption that 100% catalyst was immobilized. The BZ reactants for all experiments are aqueous solutions of sulfuric acid (J. T. Baker, Philipsburg, NJ) (0.25 M), malonic acid (Sigma-Aldrich, Milwaukee, WI) (0.025 M), and sodium bromate (0.25 M) (Sigma-Aldrich, Milwaukee, WI), which are typical excitable systems based on previous experiments by Maselko *et al.* [11,15,16].

In our experiments, an amount of 10 g of polystyrene ion exchange resin beads [11] was added to 50 mL of the BZ reactants in which the percentage of active beads ϕ was varied from 0.2 to 1. In detail, active beads, inactive beads, and 50 mL of the BZ reactants were well mixed and the beads precipitated. The mixture was placed in a 9-cm-diameter beaker. The thickness of bead bed was about 5 mm and the depth of the reactants plus the beads, about 1.5 cm. The size of the beads was between 75 to 150 μm. A camera installed 1.5 m directly above the beaker took images every 10 s in a dark room maintained at 15 °C. The wavelength of the observed wave in the beads layer is about 2 mm. Three-dimensional effects might affect the dynamics of the waves, but were not explored in our experiments.

*qingsheng.wang@okstate.edu
†Corresponding author; cheng@chemail.tamu.edu

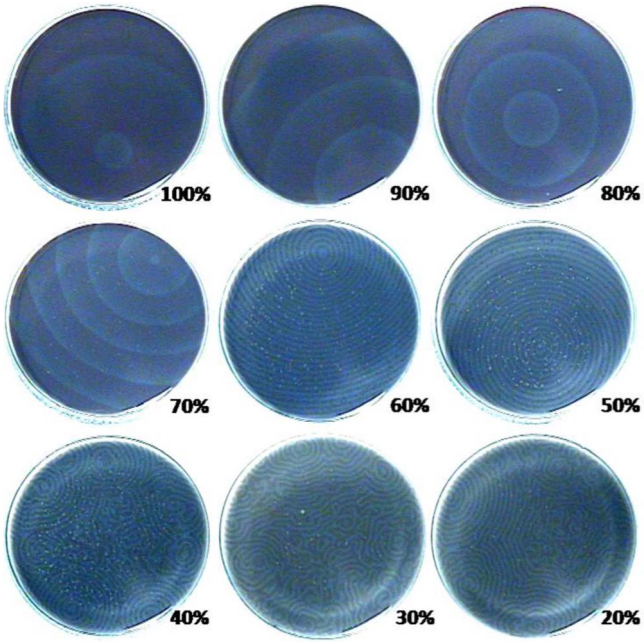

FIG. 1. (Color online) The BZ wave patterns change from targets to spirals with the reduction of the number of active beads. The percentage of active resin beads are labeled in the right bottom corner. Image sizes are 9 cm in diameter.

III. RESULTS

BZ wave patterns were generated at various active bead percentages ϕ. The snapshots of the steady wave patterns at about 2 h after the start of each experiment are displayed in Fig. 1. Target wave patterns were observed for $\phi \geq 0.7$. In the range of $0.5 \leq \phi \leq 0.6$, target waves were formed, but the wave crests close to the center were irregular and the whole pattern became noncircular. For $\phi \leq 0.4$, multiple wave initiation sites and various wave patterns coexisted, and rotating spirals were generated. No wave pattern was observed for $\phi=0.1$. The composition of inactive resin beads $(1-\phi)$ seems to act as a dynamic bifurcation parameter. As ϕ decreases, steady state of the system makes a transition from targets to spirals, separated by a transient region. It should be noted that this pattern transition is due to the percentage of inactive resin beads, not to the decrease in total concentration of the catalyst. Control experiments for different concentrations of catalyst in the samples indicated that the wave pattern transition took place at the same composition of inactive beads (ϕ between 0.5 and 0.6).

It is worth noting that a unique pattern was generated in the experiments carried out at $\phi=0.3$. Instead of multiple initiating sites and multiwaves, as shown in Fig. 1, a wave pattern originating from a high-frequency pacemaker occupied the entire area in this particular experiment about 5 h after the start of the experiment, as shown in Fig. 2(a). At the wave center, the wave crest appeared as a closed line. However, its shape deviated from the circular. The time sequence of this experiment is shown in Fig. 2(b). Due to the presence of the inactive beads occupying 70% of the total beads, the continuity of the wave was destroyed, and three separate activated pieces can be identified [insets of Fig. 2(b)]. These

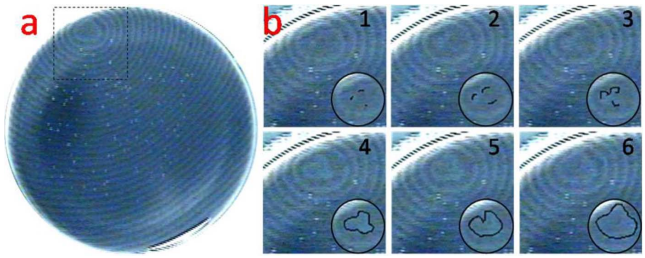

FIG. 2. (Color online) The closed wave pattern at $\phi=0.3$. (a) The closed irregular wave pattern at the steady state with a pacemaker near the edge. (b) The periodic process of generating the closed irregular pattern through the joint of three wave segments. The image sizes are about 2.9 cm in side length. Time separation between sequential frames is 40 s. The insets at the bottom-right corners illustrate the central portion of the wave.

pieces grew into three wave segments as they moved away from the center. The segments tended to curve, as shown in Fig. 2(b) and panel 3, and grow into spiral pairs [see Fig. 3(a) and panel 1]. However, the distance between the segments was too small for full development of spirals. Instead, they quickly met and joined into a closed wave pattern, which was different from the target waves observed for $\phi > 0.7$.

Bound spiral pairs were observed for samples at $\phi=0.2$, where the wave segments were further separated and allowed to become fully developed spiral waves, as shown in micrograph 1 of Fig. 3(a). However, such bound states are metastable: the two spirals in one pair have opposite topological charges and likely repel each other [17,18]. The higher-frequency spiral in the pair could expand faster and take over the other spirals, as we observed in the time sequence of Fig. 3(a). We also observed that the dynamics of spirals are peculiar due to the presence of inactive clusters, as shown in Fig. 3(b). Here the clusters were formed by the aggregation of inactive resin beads at $\phi=0.2$. Within one period of the spiral rotation, the center of the single spiral first sprouts out a closed geometric pattern composed of wave segments [Fig. 3(b), (2)]. The closed pattern expands with upward growth [Fig. 3(b), (3)], then expands horizontally, forming a semicircle on the left half [Fig. 3(b), (4)]. Meanwhile, the semicircle starts to rotate in the clockwise direction together with the whole spiral pattern [Fig. 3(b), (4) and (5)], and the

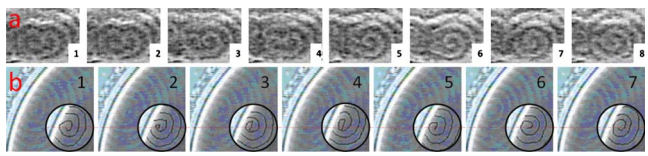

FIG. 3. (Color online) The spiral-wave patterns at $\phi=0.2$. (a) The evolution of a bound spiral pair (micrograph 1) to a single spiral (micrograph 8). The image sizes are about 1.65 cm in width. (b) Rotation of a single spiral. The side length of the image is about 2.65 cm. Insets illustrate the center of the spiral wave. Frames 1 and 7 are the beginning and end of a spiral rotation period, respectively. The time separations between sequential frames for line (a) and (b) are both 30 s.

closed segments open up. Finally, the last straight segment with the free end and curves rotates [Fig. 3(b), (6) and (7)], setting the stage for the next period. This behavior was distinctly different from that of a continuously processing spiral.

IV. DISCUSSION

When $\phi=1$, every bead in the system is able to be excited, generating a perfect target pattern. When ϕ starts to decrease, some of the beads are not active in the BZ reaction and the propagation of the waves is affected. The waves are hence generated with shorter wavelength and higher frequency due to the change of ϕ, which is consistent with theoretical predictions [19,20]. An effective medium theory has been developed by Alonso *et al.* [20] for spatially heterogeneous nonlinear reaction-diffusion media, which are similar to our case. The observed wavelength reduction, the wave pattern formation, and transition may be explained by the interplay between nonlinear reaction kinetics and diffusion.

Just below $\phi=0.6$, the percentage of inactive beads reaches a critical level at which they tend to form clusters that function as obstacles to wave propagation [21,22]. Distorted target patterns are observed in the beaker due to inactive beads hindering wave propagation, as shown in Fig. 1 for $\phi=0.6$ and 0.5. The wave crests closer to the center exhibit an unsmoothed edge and an eccentricity of about 0.6. The roughness disappears as waves propagate away from the centers, with eccentricity decreasing to 0.3. Therefore, the discrete system steps into a new regime as ϕ reduces below 0.6, which we call it transient region.

As ϕ further decreases below 0.4, instead of only one pacemaker dominating, multiple initiation sites are generated, as shown in the bottom row of Fig. 1. This new regime is called the spiral region, due to the tendency toward spiral formation. The formation of spiral pairs starts from a short wave segment, as previous theory hypothesized [23]. However, the ability to form spirals also depends on the distance between the segments, which is why spiral pairs are not observed until $\phi=0.2$. These observations confirm the theoretical prediction by Meron *et al.* and van der Deijl *et al.* [23,24].

Figure 4 depicts the measured characteristics of the wave pattern from the captured image series in Figs. 1–3. In Fig. 4(a), we can define three regions based on the wave patterns obtained in Fig. 1: target region, transient region, and spiral region. We can also see that the period of the waves decreases until it reaches the transient region. When ϕ is reduced from 1.0 to 0.7, the propagation velocity of the waves decreases linearly, as shown in Fig. 4(b). Wave characteristics show significant changes between 0.4 and 0.7. We define the lower boundary of the transient region to be $\phi_{lower}=0.48\pm0.01$ by polynomial curve fitting in Fig. 4(b) to locate the lowest velocity composition. The measured dispersion curve (velocity versus period) is plotted in Fig. 4(c), showing a decreasing wave period as propagation velocity decreases, which is consistent with previous theories [25,26]. The inactive beads, therefore, which slow the wave propagation speed, will produce high-frequency waves. Correspondingly, the wavelength decreases with ϕ, as shown in Fig. 4(d). We define the upper boundary for the transient region as $\phi_{upper}=0.59\pm0.01$ by linear fittings depicted in Fig. 4(d). Lee reported a wave pattern selection between spiral and circular pacemaker waves with a FitzHugh-Nagumo reaction-diffusion model when the parameters of homogeneous excitable media change [27]. In our work, the observed wave pattern transition between spirals and targets took place when the structure of the media changed. Future theoretical considerations might explore the structure dependence of the BZ reaction parameters [28].

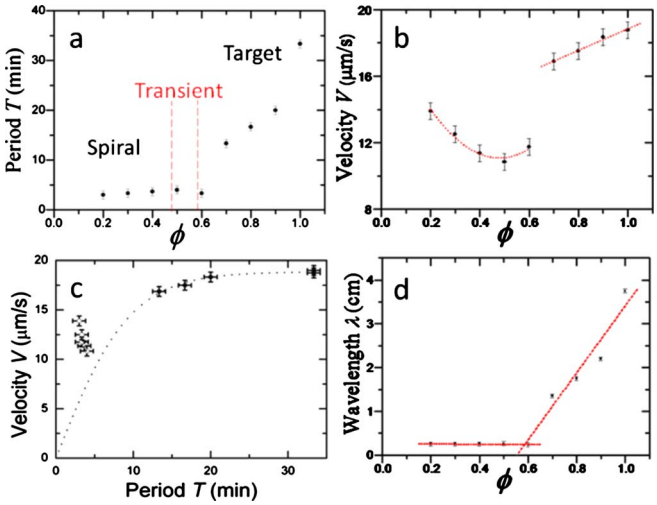

FIG. 4. (Color online) The characteristics of BZ waves vary with the composition of active beads ϕ. (a) Period of the waves. Dashed lines indicate the boundaries of the target patterns to spiral patterns transition as ϕ decreases. (b) Propagation velocity of the waves. Dotted lines are the linear fitting to the data for $\phi\geq0.7$ and polynomial fitting to the data $\phi\leq0.6$, respectively. (c) Dispersion of the waves. The dashed curve is the fitting to the data $\phi\geq0.7$ of $V=(18.87\pm0.12)^{*}\tanh[T/(9.52\pm0.35)]$. (d) Wavelength of the waves. The dotted lines are the linear fitting to the data $\phi\geq0.7$ and $\phi\leq0.6$, respectively.

V. CONCLUSION

In summary, we have developed a model of a discrete excitable medium in which the population of inactive resin beads acts as the bifurcation parameter that controls the wave pattern transition from targets to spirals. The behavior of bound spiral pairs and their separation is indicative of the effect of inactive clusters, which break the wave into segments and allow them grow into spiral pairs. Because heterogeneities are intrinsic in biological systems, this model system might be applied to the understanding of the occurrence of the spiral wavelets in the heart with diseased cells. Future work will include computer simulations of this heterogeneous model system and various wave pattern transition phenomena in a broad range of BZ reaction conditions.

ACKNOWLEDGMENTS

M.M. gratefully acknowledges partial funding for this work from University of Malaga (Junta de Andalucia), Project P09-TEP-5369 with Prof. Ignacio Loscertales. This work is partially supported by the start-up funds from Department of Chemical Engineering at Texas A&M University.

[1] J. M. Davidenko, A. V. Pertsov, R. Salomonsz *et al.*, Nature (London) **355**, 349 (1992).
[2] N. A. Gorelova and J. Bures, J. Neurobiol. **14**, 353 (1983).
[3] J. Lechleiter, S. Girard, E. Peralta *et al.*, Science **252**, 123 (1991).
[4] F. Sagues, J. M. Sancho, and J. Garcia-Ojalvo, Rev. Mod. Phys. **79**, 829 (2007).
[5] A. S. Mikhailov and K. Showalter, Phys. Rep. **425**, 79 (2006).
[6] F. Sagues and I. R. Epstein, Dalton Trans. 2003, 1201.
[7] G. Bub, A. Shrier, and L. Glass, Phys. Rev. Lett. **94**, 028105 (2005).
[8] M. Assenheimer and V. Steinberg, Nature (London) **367**, 345 (1994).
[9] A. F. Taylor, M. R. Tinsley, F. Wang *et al.*, Science **323**, 614 (2009).
[10] J. M. Greenberg and S. P. Hastings, SIAM J. Appl. Math. **34**, 515 (1978).
[11] J. Maselko, J. S. Reckley, and K. Showalter, J. Phys. Chem. **93**, 2774 (1989).
[12] K. H. W. J. ten Tusscher and A. V. Panfilov, Phys. Rev. E **68**, 062902 (2003).
[13] K. H. W. J. ten Tusscher and A. V. Panfilov, Europace **9**, vi38 (2007).
[14] R. F. Gilmour, Drug Discovery Today **8**, 162 (2003).
[15] J. Maselko and K. Showalter, Nature (London) **339**, 609 (1989).
[16] J. Maselko and K. Showalter, Physica D **49**, 21 (1991).
[17] M. Ruiz-Villarreal, M. Gomez-Gesteira, C. Souto, A. P. Munuzuri, and V. Perez-Villar, Phys. Rev. E **54**, 2999 (1996).
[18] F. Xie, Z. Qu, J. N. Weiss, and A. Garfinkel, Phys. Rev. E **63**, 031905 (2001).
[19] B. E. Steinberg, L. Glass, A. Shrier G. Bub, Philos. Trans. R. Soc. London, Ser. A **364**, 1299 (2006).
[20] S. Alonso, R. Kapral, and M. Bar, Phys. Rev. Lett. **102**, 238302 (2009).
[21] A. Babloyantz and J. A. Sepulchre, Physica D **49**, 52 (1991).
[22] J. A. Sepulchre and A. Babloyantz, Phys. Rev. Lett. **66**, 1314 (1991).
[23] E. Meron and P. Pelce, Phys. Rev. Lett. **60**, 1880 (1988).
[24] G. B. M. van der Deijl and A. V. Panfilov, Phys. Rev. E **78**, 012901 (2008).
[25] J.-M. Flesselles, A. Belmonte, and V. Gaspar, J. Chem. Soc., Faraday Trans. **94**, 851 (1998).
[26] J. D. Dockery, J. P. Keener, and J. J. Tyson, Physica D **30**, 177 (1988).
[27] K. J. Lee, Phys. Rev. Lett. **79**, 2907 (1997).
[28] O. Steinbock, P. Kettunen, and K. Showalter, Science **269**, 1857 (1995).